How can Removethe Earth Dam's Cracks during the Strong Earthquake by Isolated Damping Layer System

BehrouzGordan[1], Azlan Adnan[2]

1- Engineering Seismology and Earthquake Engineering Research Group (e-seer), UniversitiTechnologi Malaysia
81310 Skudai, Johor, Malaysia

2- Engineering Seismology and Earthquake Engineering Research Group (e-seer), UniversitiTechnologi Malaysia
81310 Skudai, Johor, Malaysia
Email:bh.gordan@yahoo.com

Abstract

The effect of blanket layer using an Isolator Damping layer (IDL) between river sand foundation and short embankment to eliminate damage under severe earthquake was investigated in the present study. In the case of numerical analysis by ANSYS program, dominant frequency (DF) was calculated by free vibration analysis. Soil mechanic tests of thirteen samples were carried out to design the IDL formula. In terms of critical condition for seismic effect such as resonance, five physical small modelingswere tested using vibrator table under the dominant frequency with the scale parameter 1/100. As a result, the dam was significantly damaged without a blanket layer IDL. In order to reduce damage, the best performance was observed using blanket layer (IDL) when this layer was extended below the reservoir region. The size of reinforced thickness layer is one fourth of dam height. This method is a new suggestion for the design of an earth dam in seismic zones.

Keywords: Dominant frequency, Vibrator table, Physical modeling, Damping, Damage

1. INTRODUCTION

The dynamic assessment of earth dams has been dramatically started after the observation of some damages during the severe earthquake. In this domain, huge damages such as body cracks were recorded. Totally, this knowledge is corresponded to control dam behavior to avoid of failure process. Besides, the earth dam construction is possible with respect to compaction process. Therefore, the consolidation settlement can be completely maximized at the end of construction. In terms of earthquake effect on dam response, the first phase of total settlement is related to the final static displacement. Therefore, the total settlement is the superposition of static and dynamic effect. According to a literature review in this study, a few cases of data monitoring were just recorded (Segal et al 1992, Gikas et al 2008, Verdugo et al 2012). Two cases such as the lack of data monitoring and technological development to provide a computing program that is led to use numeric method for dynamically analyzing. In the other words, the numerical analysis was commonly utilized in several studies to predict the dynamic behavior during the earthquake (Parish et al 2009, Berhe at al 2010, Xia et al 2010, Kong et al 2010, Bayraktar et al 2011, Risheng et al 2006). In terms of analysis technique, two methods such as Finite-Element (FEM) and Finite-Difference (FDM) can be applied. Dynamic analysis of earth dam was carried out by using two techniques such as two-dimensional and three-dimensional (Elgamal 1992, Gordan& Adnan 2013, Papalou et al 2001, Yu et al 2005). To select, plane strain (2D) and plane stress (3D) depends on dam configuration and valley shape in order to distribution of lateral strain (Mejia et al 1983). In terms of reinforcement methods, some methods have been used to reinforce the dam in order to improve dynamic behavior along the earthquake (Borges 2014, Yildiz 2009, Le at al 2009, Abusharar et al 2009, Noorzad et al 2010). To verify results based on numeric analysis, both tests such as shaking table and centrifuge were successfully experienced (Matsumaru et al 2008, Namdar et al 2010, Wang et al 2011). However, to avoid dam failure by earthquake, the effect of foundation soil was the significant role to generate cracks with respect to increase acceleration and displacement at the crest. In the present study, the main purpose is the improvement of dam performance under severe motion like the resonance condition using blanket layer between foundation and homogenized earth dam. In other words, this paper presents a novel method to remove damage by using new material (IDL). In order to discuss about the damage level of the dam, five physical models in regards to dominant frequency will be vibrated. To improve dam performance, the optimum thickness will be finally suggested.

2.0 LABORATORY SOIL TESTS

Two types of experimental tests were carried out in this study. Firstly, soil mechanic tests were performed based on British Standard (BS) in order to design isolator damping layer (IDL), (Gordan&Adnan 2014). Secondly, some small scale models with respect to find the best location to reinforce the dam were vibrated by using vibrator table.In terms of soil characters, the British Standard (BS) for soil mechanic tests was used. Based on soil classification, the local laterite soil MH was applied. The summarizing of laterite properties illustrated in Table 1, as used in this study. Moreover, Table 2 shows samples with respect to different mixtures to design IDL.

Table 1. Characteristics of the laterite soil for dam body.

Physical properties	Value	Physical properties	Value
Specific gravity	2.40	Unconfined compressive strength (KPa)	306.26
Liquid limit, LL (%)	75	Cohesion (KPa)	25.18
Plastic limit, PL (%)	41	Angle of internal friction (Degree)	30.00
Plasticity index, PI (%)	34	Modulus elasticity (KPa)	15283.72
BS classification	MH	Coefficient of Volume Compressibility (m_v, m2/MN)	0.1055
Maximum dry density (g cm-3)	1.33	Coefficient of Consolidation (cv, m2/yr)	44.16
Optimum moisture content (%)	35	Permeability (cm/seconds)	1.29E-5

Table 2. Sample definition to design Isolated Damping Layer (IDL), Laterite with Tire Driven Aggregate (TDA) and Micro silica

Sample number	Component	Sample number	Component
1	Laterite	8	Laterite+5%TDA+2% Silica
2	Laterite+3%TDA	9	Laterite+5%TDA+3% Silica
3	Laterite+5%TDA	10	Laterite+7%TDA+3% Silica
4	Laterite+7%TDA	11	Laterite+7%TDA+4% Silica
5	Laterite+10%TDA	12	Laterite+10%TDA+4% Silica
6	Laterite+3%TDA+2% Silica	13	Laterite+10%TDA+5% Silica
7	Laterite+3%TDA+3% Silica		

Based on soil test as carried out by Gordan&Adnan on 2010, Sample number 10 was selected with respect to excellent performance. Furthermore, in order to estimation of damping ratio, the nonlinear stress–strain characteristics of soils (Figure 1- a), for analysis purposes, can be represented by bilinear relationships (Figure 1-b) or multi-linear relationships. However, the use of an equivalent linear Visco-elastic analysis leads to similar results. The damping ratio depends on both areas as can be seen with blue and red color in this Figure (Das 2013). This ratio can be given by Eq.1.

$$\text{Damping ratio} = D = (1/4\pi)^* \text{ (Loop area/ area under stress strain curve)} \quad (1)$$

However, the area under the stress-strain curve and the hysteresis loop area can be computed according to Figure 1. Figure 2 shows the damping ratio for sample 1 and sample 10, respectively. It can be seen that this ratio was 17.95% in laterite soil. In terms of soil improvement, the damping coefficient increased to 22.63% for sample 10 (7%TDA with 3% Silica).

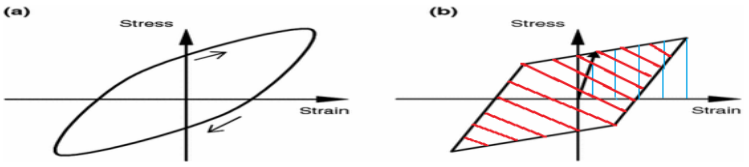

Figure 1. Damping definition, hysteretic and equivalent bilinear stress–strain relationships for soil: a stress–strain curves; b bilinear idealization (Seed et al 1986)

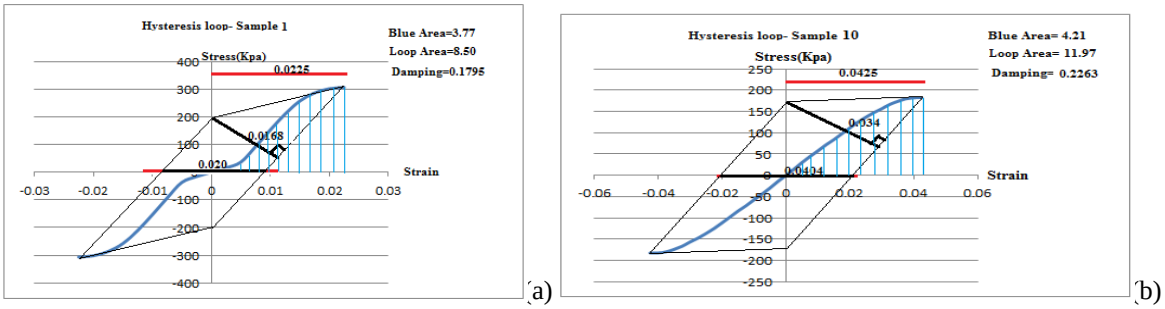

(a) (b)

Figure 2. Estimation of damping ratio, a) sample 1, b) sample 10

After discussion about all tests on soil mechanic that carried out, sample 10 shows the excellent performance in order to reinforce the dam. Therefore, IDL material was defined by using sample 10. In the physical small dam modeling, this material to reinforce dam in different location was used. For small-scale modeling, the river sand was used for the foundation. Table 3 presents sand properties as used for foundations. It is important to note that, river sand included uniform size particles because uniformity coefficient was less than five. In addition, the coefficient of curvature was less than one. The soil is said to be well graded if this value in order to avoid of liquefaction phenomena, lies between one and three. Therefore, this type of sand was selected in order to critical condition for the foundation.

Table 3. Sand properties for dam foundation.

Physical properties	value	Physical properties	value
Specific gravity	2.547	Density for I_d=75% (gr/cm^3)	1.613
Cohesion (KPa)	0.00	Permeability (cm/s)	0.1
Angle of internal friction (Degree)	35	Maximum size(mm)	2.00
Modulus elasticity (KPa)	32460	Minimum size(mm)	0.075
Maximum dry density (gr/cm^3)	1.72	Uniformity coefficient C_u	4.375
Minimum dry density (gr/cm^3)	1.36	Coefficient of curvature C_c	0.97

3.0 SMALL SCALE MODEL ON VIBRATOR TABLE

Physical models with scale parameter equal 1/100 were tested. In order to research methodology for this purpose, some aspect included characteristic of vibrator table, displacement transducer, data logger, sinusoidal motion, scale parameter for static or dynamic condition, free vibration analysis and physical modeling will be presented. In this study, five small-scale dam were tested, as will be explained in next section.

3.1 Vibrator table

In this study, vibrating table 24-9112 (CN-166) with respect to sinus motion was used. Figure 3 shows the vibrating desk that was cushioned steel and semi noiseless electromagnetic vibrator with 3600 vpm operating frequency. In addition, it has a separate controller to vary vibrator amplitude in case of frequency capacity limit to 100 Hz. Table capacity was equal to 750 lbs (340 kg). Double amplitude range was located at 0.002 inch (0.05 mm) to 0.015 inch (0.38mm). Actuator was an electromagnetic vibrator over 100 lbs (45.30kg). The table was square shape 30 inch (762 mm). The table thickness was 33.3mm of steel. In case of weight, it was net 555 lbs (252 kg) and shipping 605 lbs (274 kg). Figure 3 illustrates the vibrator table for this study.

Figure 3. Vibrator Table

3.2 Displacement transducer and data logger

Displacement transducer CDP-D was utilized with respect to dual isolated I/O ports. By using transducer, one set of cables for input and output were connected to the analog measuring instrument and other set to the digital measuring instrument. With two different types of measuring equipment connected to this transducer, simultaneous measurements can be made without interference. Figure 4-A shows the displacement transducer and Figure 4-B shows the dimensions for transducer CDP-100. To measure displacement at both edges of the crest in small-scale modeling, two transducers were installed. In terms of data record, data logger or data recorder is an electronic device that records data over time or in relation to location either with a built in instrument or sensor or via external instruments and sensors.

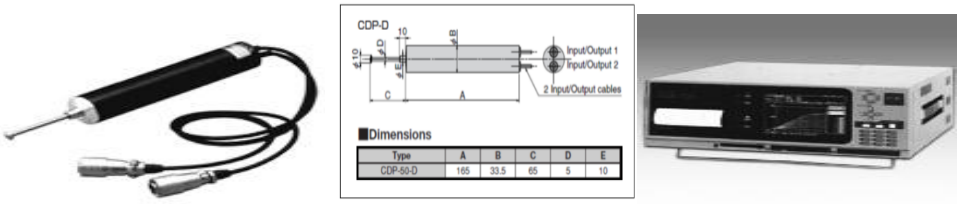

(a) (b) (c)

Figure 4. Transducer and data logger, a) Displacement transducer, CDP-100, b) Dimension of displacement transducer (CDP-100) and c) Data logger, UCAM-70A

Figure 4-C illustrates the data logger that used in this study. Based on device ability, results were printed during the vibration duration. After that, results were classified by using Excel program. It should be noting that, both

transducers as mentioned previously were connected to this data logger (UCAM-70A) in order to record vertical displacement during the vibration. In addition, the sub step of vibration period was equal two seconds based on device ability with respect to print.

3.3 Sinusoidal vibrate loading

There is a mathematical relationship between frequency, displacement, velocity, and acceleration for sinusoidal motion according to consider the peak value for them. The relationship is such that if any two of the four variables are known, the other two can be calculated. Table 4 shows all equations that provided in this context (Griffin 2012)

Table 4. Conversion for peak value in sinusoidal motion, Displacement (x), Velocity (V), Acceleration (A), and Frequency (f)

	Displacement, x	Velocity, V	Acceleration, A
Displacement, X	X=X	$X=\frac{V}{2\pi f}$	$X=\frac{A}{(2\pi f)^2}$
Velocity , V	V=2πfX	V=V	$V=\frac{A}{2\pi f}$
Acceleration, A	$A=(2\pi f)^2X$	A=2πfV	A=A

G in these formulas is not gravity acceleration. It is a constant for calculation within different systems. Respectively, for metric, imperial and Si G is 9.80665m/s², 386.0885827 in/s² and is 1.00 m/s².

Since the motion is sinusoidal, the displacement, velocity, and acceleration are changing sinusoidal trend. However, they are not in the same phase. The phase relationship between displacement, velocity, and acceleration is that such that velocity is 90° out of phase with acceleration and displacement is 180° out of phase with acceleration.

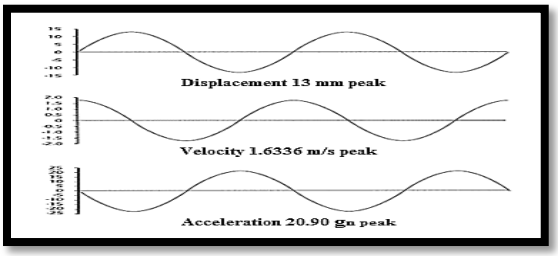

Figure 5. Sinusoidal motionfor 20 Hz.

In other words, when displacement is at a maximum, velocity is at a minimum, and acceleration is at a maximum. It should be noting that, 1 g_n = 9.80665 m/s² = 32.174 ft/s² = 386.0886 in/s². Figure 5 shows the example of displacement distribution with velocity and acceleration while the frequency of sinusoidal motion is twenty hertz.

3.4 Scaling laws

In case of the scale parameter, the scale factor can be used according to Eq.1.

$$x^* = \frac{x_m}{x_p} \tag{2}$$

The subscript m represents "model" and the subscript p represents "prototype" and x^*represents the scale factor for the quantity x (Garnier et al 2007)

The reason for spinning a model on a centrifuge is to enable small-scale models to feel the same effective stresses as a full-scale prototype. This goal can be stated mathematically as

$$\sigma'^{x} = \frac{\sigma'_m}{\sigma'_p} = 1 \tag{3}$$

Where the asterisk represents the scaling factor for the quantity, σ'_m is the effective stress in the model and σ'_p is the effective stress in the prototype.

In soil mechanics the vertical effective stress, σ' for example, is typically calculated by

$$\sigma' = \sigma^t - u \tag{4}$$

Where σ^t and u are total stress and pore pressure, respectively. For a uniform layer with no pore pressure, the total vertical stress at a depth H may be calculated by:

$$\sigma^t = \rho g H \tag{5}$$

Where ρ represents the density of the layer and g represents gravity. In the conventional form of centrifuge modeling (Garnier et al 2007), it is typical that the same materials are used in the model and prototype; therefore, the densities are the same in model and prototype, i.e.

$$\rho^* = 1 \tag{6}$$

Furthermore, in conventional centrifuge modeling all lengths are scaled by the same factorL^*. To produce the same stress in the model as in the prototype, we thus require

$$\rho^* g^* H^* = 1 \; g^* L^* = 1 \tag{7}$$

It may be rewritten by Eq.8.

$$g^* = \frac{1}{L^*} \tag{8}$$

The above scaling law states that if lengths in the model are reduced by some factor, n, then gravitational accelerations must be increased by the same factor, n in order to preserve equal stresses in model and prototype.

For dynamic problems where gravity and accelerations are important, all accelerations must scale as gravity is scaled, i.e.

$$a^* = g^* = \frac{1}{L^*} \tag{9}$$

Since acceleration has units of $\frac{L}{T^2}$, it is required that

$$a^* = \frac{L^*}{T^2} \tag{10}$$

Hence, it is required that:

$$\frac{1}{L^*} = \frac{L^*}{T^2}, \text{ or } T^* = L^* \tag{11}$$

Frequency has units of inverse of time, velocity has units of length per time, so for dynamic problems we also obtain

$$f^* = \frac{1}{L^*} \tag{12}$$

$$v^* = \frac{L^*}{T^*} = 1 \tag{13}$$

For model tests involving dynamics, the conflict in time scale factors may be resolved by scaling the permeability of the soil (Garnier et al 2007).

3.5 Free Vibration Analysis and Dominant Frequency

In dynamic assessment, free vibration analysis is the base of study for dynamic analysis. In fact, the distribution of frequency in the different vibration mode can be computed by the application of modal analysis based on Finite-Element Method (FEM). It worth mentioning that, this analysis is perfectly related to the mass and spring. In case of the mass–spring–damper system, the first assumption is negligible about damping effect. Therefore, there is not any external force on mass in this state. The force applied to the mass by the spring is proportional to the amount of the spring is stretched "x" (It can be assumed that spring is already compressed due to the weight of the mass. In terms of numerical analysis, modal analysis was carried out by using ANSYS program in this study to compute dominant frequency for small-scale model regarding 3D analysis. This program is one of the famous software with respect to Finite- Element Method (FEM). In particular, this software is one of the universal programs with high level of the ability for different analyses. A strong ability to compute free vibration analysis is possible with modal analysis (Fluent 2009).In order to select element based on Help menu, solid 8 nodes 183 (3D) was used for this purpose. Figure 6 shows the mapped mesh for numerical modeling. In this figure, 23956 elements and 35457 nodes in models were used for free vibration analysis. According to this condition, free vibration analysis to access frequency in different vibration modes was carried out, as results can be discussed in the next section.

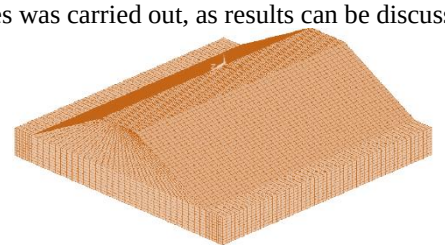

Figure 6. Free mesh

In terms of modal analysis, the free vibration analysis was calculated by ANSYS program. Figure 7 shows displacement in three directions of model and total displacement in the first vibration mode. Because, based on distribution of frequency in the first mode to fifth mode, it is important to note that, the minimum frequency (0.22986Hz) was observed in the first vibration mode. It means that, the vibration period was maximum and critical in this mode.

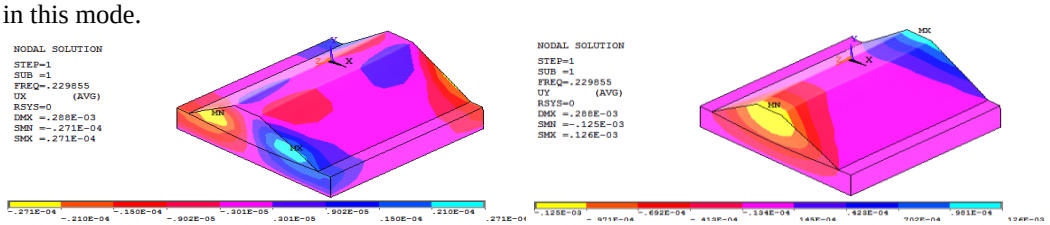

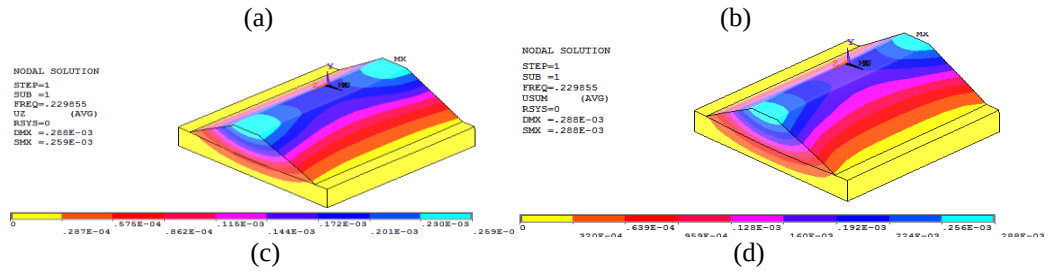

Figure 7. Mode shape 1, a) Horizontal displacement, b) Vertical displacement, c) Lateral Displacement. d) Total displacement

Distribution of frequency in different vibration mode indicated that, this value was respectively obtained 0.26257 Hz, 0.28387 Hz and 0.30135 Hz in the vibration shape mode 2 until 4.

4.0 RESULTS AND DISCUSSION

In order to find the best location of reinforcement in dam, five small dam with different location of reinforcement using IDL material was vibrated by dominant frequency (22.986 Hz) with respect to resonance condition. Figure 8 shows five small-scale dam (Model A, B, C and D), it is obvious that models have a same dimension. In this Figure, the reinforced area illustrated with a hatch area. For example, model D indicated that all dam body was reinforced. For this purpose, one steel box for modeling was used. This box made by five sheets of Plexiglas with 20mm thickness. One of them was in the base of model. The level of reservoir was 75% of the dam height. The scale parameter was 1/100. It means that model was one hundred times smaller than prototype. The dam height was 22.7 meter in reality but it was made 22.7 cm in physical model. In addition, small-scale modeling was coupled by foundation. Foundation material was dense sand with 75% relative density. Sand properties was mentioned in soil mechanic test. Figure 9 shows some details including dam perspective, soil compaction, network index and reservoir. In this Figure, two LVDT on the middle of model at the both edges of the crest was installed. In order to support, one steel frame and one steel beam were applied (See Figure 9.A). However, both LVDT were connected to data logger device by specific cables. In terms of compaction soil for each layer, the steel roller was used that selected by trial error method. Wood molding with respect to control slope via network index was used. In order to avoid absorption of soil water content, both the described molds were just soaked by water before use. To tank purpose, small-scale models were filled up by water with very slow rate.

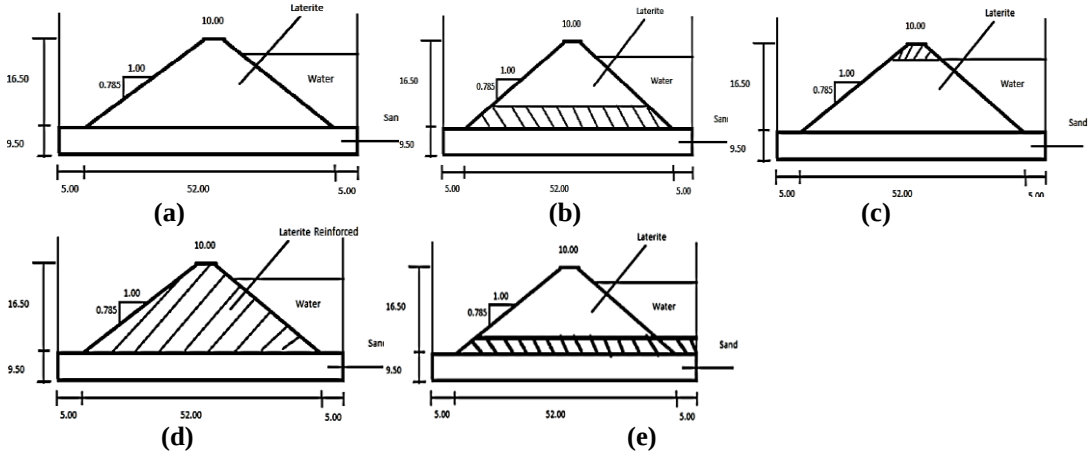

Figure 8. Model introducing (a, b, c, d and e) for small dam (cm); (S=1/100)

After vibration equal two minutes for all models, the vertical displacement for both slope such as upstream and downstream were printed. With respect to use Excel program, Figure 10 shows the distribution of vertical displacement in both edges in the middle of the crest and relative displacement in all models. It was obvious that, distribution of the vertical displacement indicated a same trend for both models such as A and E. In both models, displacement values were negative during the vibration. It means that, both of them were in uplift condition. In this Figure also, maximum and minimum peak of the relative displacement was respectively occurred in model B and C with 2.13mm and 0.06 mm. It is also worth noting that, this value was at convergence position for model A and E with 0.24mm and 0.25mm, respectively.

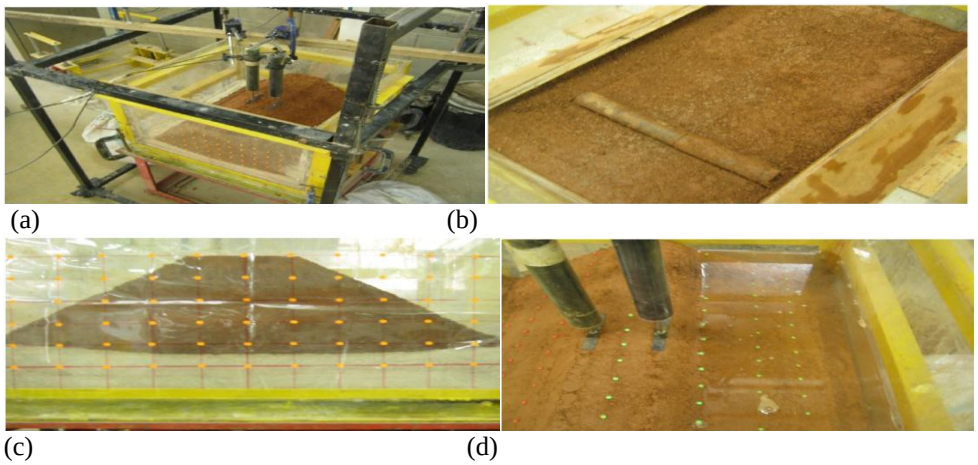

Figure 9. small-scale dam; a) Dam perspective with two LVDT, b) Soil compaction with roler, c) Dam section with index network and d) Dam with tank before vibration

In terms of damage location in models, Figure 11 shows the damage in model-A which occurred at upstream and downstream. The level of damage was greater in upstream. It was very sensible occurrence in case of hydrodynamic pressure along the vibration. Also in this Figure, the maximum longitudes cracks (See line C) were observed near to the middle of dam at the crest. In order to damage at downstream, the transverse cracks was significantly occurred in dam toe. Figure 12 shows model-B that damaged after vibration. It can be observed that, dam was significantly damaged in some locations such as crest and surfaces. Body cracks and failure process was dramatically occurred in both area near to abutments. Also in this Figure, one transverse cracks in the middle of the crest was seen (See part c). This damage was significantly repeated at upstream in model-C, but it was placed in dam toe, it can be seen in Figure 13.

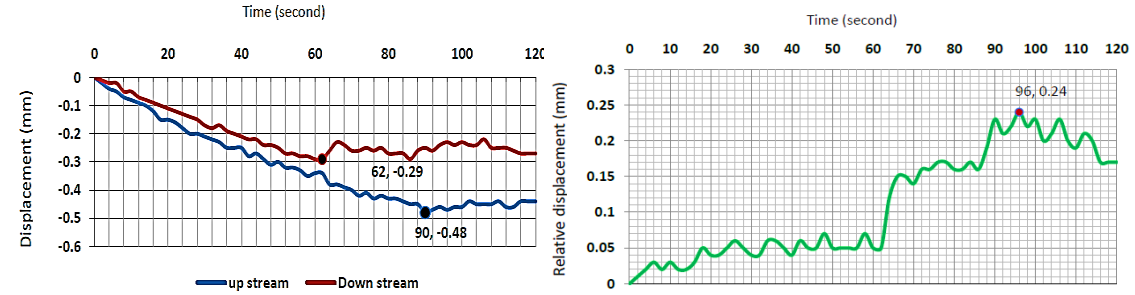

Model-a

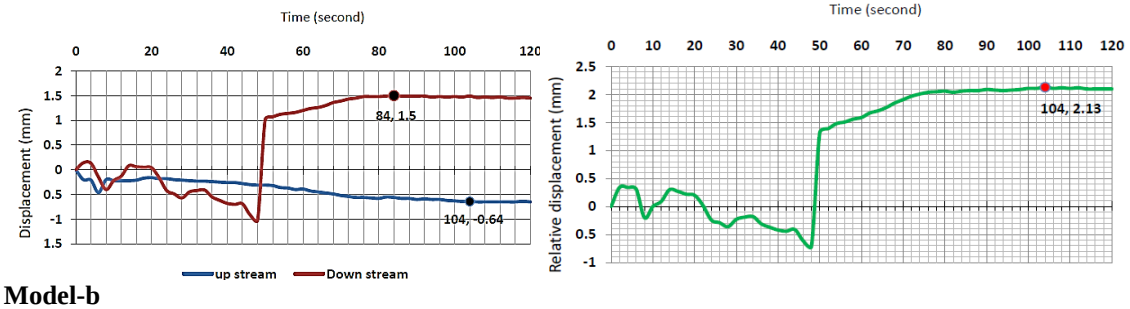

Model-b

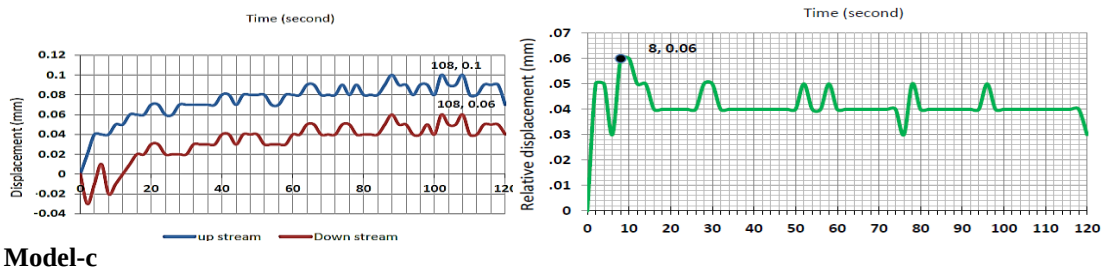

Model-c

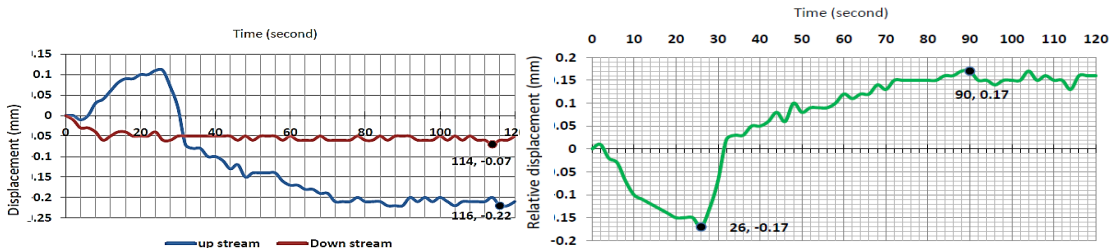

Model-d

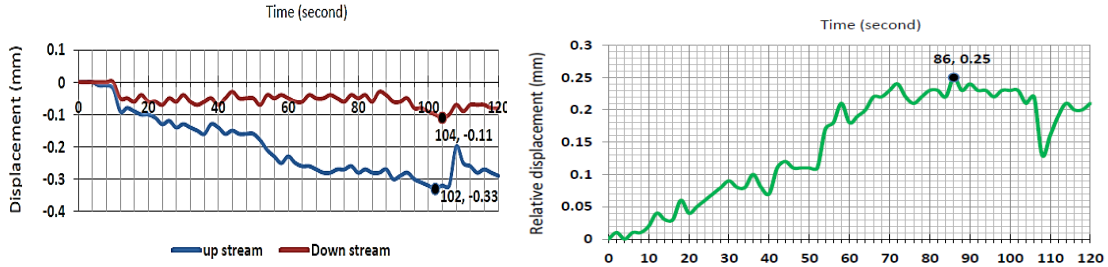

Model-e

Figure 10. The distribution of vertical displacement in both edges in the middle of the crest and relative displacement in all models

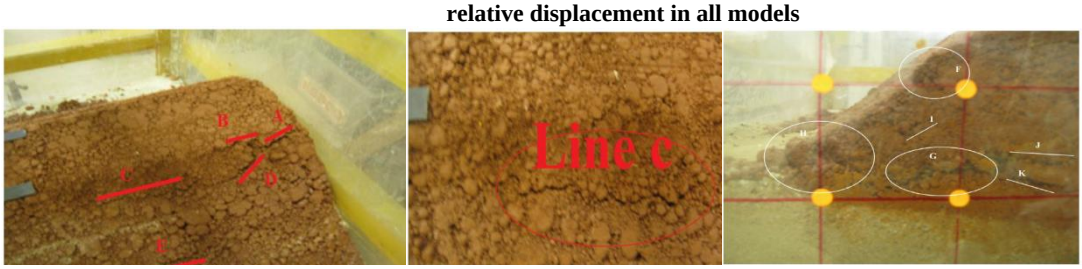

a **b** **c**

Figure 11. Damage in the first model (Model-A)

In addition, model-D was damaged in three places such as both abutments and middle of the upstream. Figure 13 shows the model-D that damaged in toe. Briefly, all four models were damaged, as discussed previously. On the other hand, a successful way in order to remove damage was obtained in model-E, as shown in Figure 14. Figure 14 shows that, model was safe after vibration without any damage. In this Figure, the reinforced blanket layer using IDL material was indicated by red circles between dam and foundation. In addition, it was very important to note that, both surfaces were safe and dam was stable under severe seismic loading like resonance motion. In fact, a good absorption of energy with respect to increase damping was found by using IDL. In case of using this technique, displacement in both edges of the crest with negative value indicated the uplift situation. Moreover, relative displacement was like to the first model.

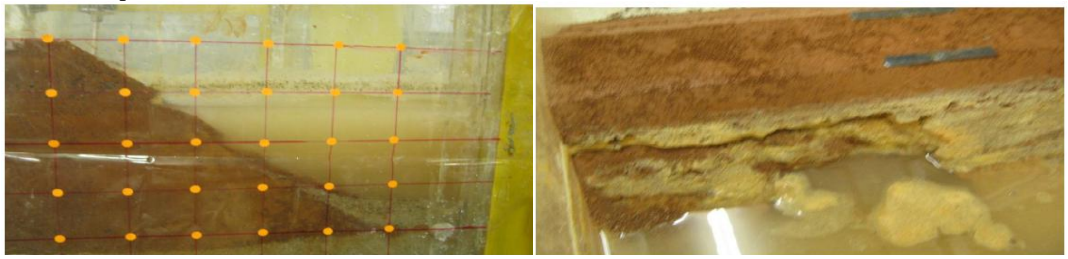

a **b**

d

Figure 12. Damage in second model (B)

Therefore, dam behavior before and after reinforcement was similar for both distributions of displacement. Nevertheless, model E was successful to remove damage with respect to high level of damping in blanket layer. In fact, this model shows the excellent performance in earth dams when the blanket layer was expanded below tank. Finally, blanket layer using Isolator Damper Layer (IDL) below dam and tank is a good recommendation for earth dams in seismic zone when reinforced thickness is one fourth of dam height. As recommends, optimization of thickness in this method is the next study.

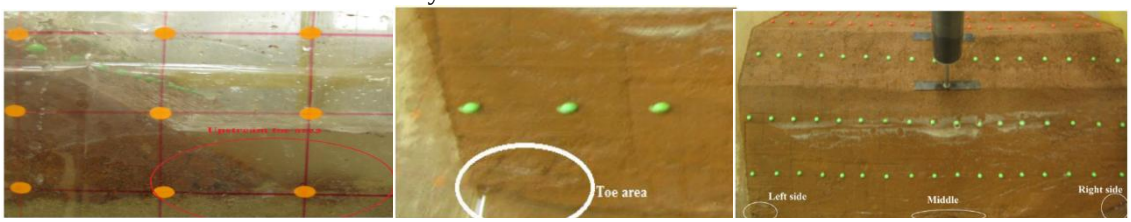

a **b** **c**

Figure 13. Damage in third model (C) for position a&b, Damage in forth model (D) for position c

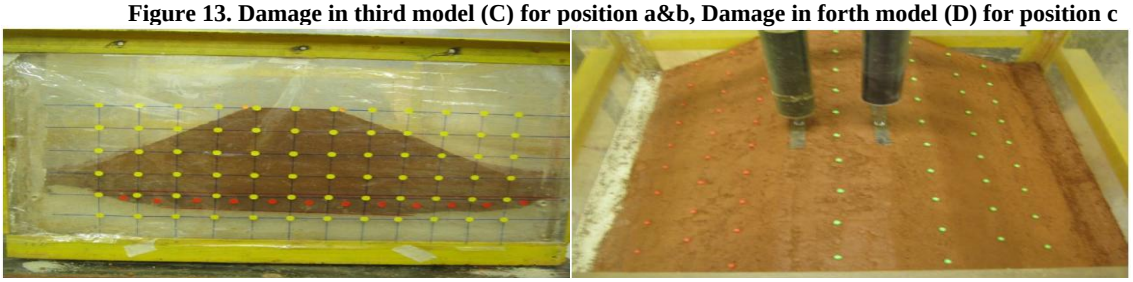

a b

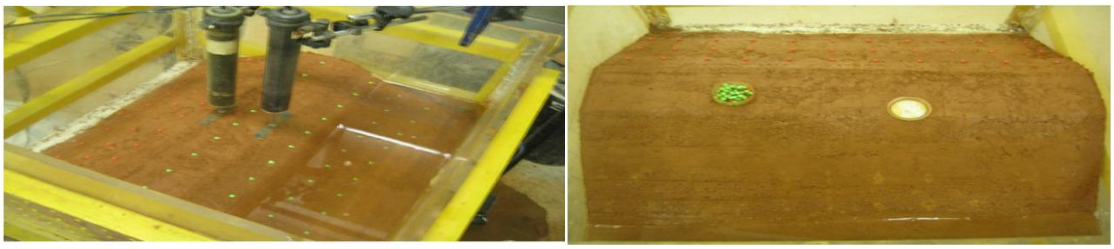

C d

Figure 14. Dam stabilization in fifth model (E)

5.0 CONCLUSION

In this study, the earth dam performance under severe seismic motion, such as resonance was evaluated by using blanket layer (IDL). With respect to soil mechanic test, the optimum mixture for IDL was designed. IDL powder was made by using some materials. Main material was a local soil (Laterite) with 90%, and additives such as TDA (Tire Driven Aggregate with 7 %), and MS (Micro Silica) with 3% was used. This material was utilized to reinforce the dam in small-scale physical modeling. According to numerical analysis, the dominant frequency (0.2298 Hz) in order to be the maximum effect of modeling vibration was computed. By using this frequency for physical modeling, the damage location and distribution of vertical displacement at the both edges of the crest in the middle of small dams for five small models with scale 1/100 was discussed. As results, the best performance in order to remove damages was obviously observed in model-E while other models were dramatically damaged in some locations such as upstream, downstream and crest. In addition, the thickness of the blanket layer in this model was one fourth of dam height. Finally, this model is a novel method to reinforce the dam under strong earthquake like resonance phenomena that recommended for earth dam design in seismic zones.

ACKNOWLEDGMENT

This study is made possible by the support of the International Doctorate Fellowship of UniversitiTeknologi Malaysia, and it is very much appreciated.

REFERENCES

Zeghal, M., & Abdel-Ghaffar, A. M. (1992).Analysis of behavior of earth dam using strong-motion earthquake records.Journal of geotechnical engineering, 118(2), 266-277.

Gikas, V., &Sakellariou, M. (2008).Settlement analysis of the Mornos earth dam (Greece): evidence from numerical modeling and geodetic monitoring. Engineering Structures, 30(11), 3074-3081.

Verdugo, R., Sitar, N., Frost, J. D., Bray, J. D., Candia, G., Eldridge, T., ...&Urzua, A. (2012). Seismic Performance of Earth Structures during the February 2010 Maule, Chile, Earthquake: Dams, Levees, Tailings Dams, and Retaining Walls. Earthquake Spectra, 28(S1), S75-S96.

Parish, Y., &Abadi, F. N. (2009).Dynamic Behaviour of Earth Dams for Variation of Earth Material Stiffness.Proceedings of World Academy of Science: Engineering & Technology, 50.

Berhe, T. G., Wang, X. T., & Wu, W. (2010).Numerical Investigation into the Arrangement of Clay Core on the Seismic Performance of Earth Dams.In Soil Dynamics and Earthquake Engineering (pp. 131-138).ASCE.

Xia, Z. F., Ye, G. L., Wang, J. H., Ye, B., & Zhang, F. (2010).Fully coupled numerical analysis of repeated shake-consolidation process of earth embankment on liquefiable foundation. Soil Dynamics and Earthquake Engineering, 30(11), 1309-1318.

Kong, X. J., Zhou, Y., Xu, B., & Zou, D. G. (2010). Analysis on seismic failure mechanism of zipingpu dam and several reflections of aseismic design for high Rock-fill dam. Earth and Space, 3177-3189.

Bayraktar, A., Kartal, M. E., &Adanur, S. (2011). The effect of concrete slab–rockfill interface behavior on the earthquake performance of a CFR dam. International Journal of Non-Linear Mechanics, 46(1), 35-46.

Risheng Park Piao, P. E., Rippe, A. H., Barry Myers, P. E., & Lane, K. W. (2006). Earth dam liquefaction and deformation analysis using numerical modeling.

Elgamal, A. W. (1992). Three-dimensional seismic analysis of La Villita dam.Journal of geotechnical engineering, 118(12), 1937-1958.

Gordan.B. &Azlan.B.A.(2013). Effect of material properties in CFRD tailing-embankment bridge during a strong earthquake. Caspian Journal of Applied Sciences Research, 2(11), pp. 61-72.

A Papalou, A., &Bielak, J. (2001). Seismic elastic response of earth dams with canyon interaction. Journal of geotechnical and geoenvironmental engineering, 127(5), 446-453.

Yu, Y., Xie, L., & Zhang, B. (2005).Stability of earth–rockfill dams: influence of geometry on the three-dimensional effect. Computers and Geotechnics, 32(5), 326-339.

Mejia, L. H., & Seed, H. B. (1983).Comparison of 2-D and 3-D dynamic analyses of earth dams. Journal of Geotechnical Engineering, 109(11), 1383-1398.

Borges, J. L. (2004). Three-dimensional analysis of embankments on soft soils incorporating vertical drains by finite element method. Computers and Geotechnics, 31(8), 665-676.

Yildiz, A. (2009). Numerical analyses of embankments on PVD improved soft clays. Advances in Engineering Software, 40(10), 1047-1055.

Le Hello, B., & Villard, P. (2009). Embankments reinforced by piles and geosynthetics—Numerical and experimental studies dealing with the transfer of load on the soil embankment. Engineering Geology, 106(1), 78-91.

Abusharar, S. W., Zheng, J. J., Chen, B. G., & Yin, J. H. (2009). A simplified method for analysis of a piled embankment reinforced with geosynthetics. Geotextiles and Geomembranes, 27(1), 39-52.

Noorzad, R., &Omidvar, M. (2010). Seismic displacement analysis of embankment dams with reinforced cohesive shell. Soil Dynamics and Earthquake Engineering, 30(11), 1149-1157.

Matsumaru, T., Watanabe, K., Isono, J., Tateyama.M. and Uchimura, T. (2008).Application of cement-mixed gravel reinforced by ground for soft ground improvement. *Proceedings of the 4th Asian Regional Conference on Geosynthetics June 17 - 20, 2008* .Shanghai, China.380-385.

Namdar, A. A. k. Pelko.Seismic Evaluation of Embankment Shaking Table Test and Finite Element Method.The Pacific Journal of Science and Technology2010 November-volume11, Number2http://www.akamaiuniversity. us/PJST. http.

Wang, L., Zhang, G., & Zhang, J. M. (2011). Centrifuge model tests of geotextile-reinforced soil embankments during an earthquake. Geotextiles and Geomembranes, 29(3), 222-232.

BehrouzGordan, Azlan bin Adnan (2014). Excellent performance of earth dams under resonance motion using isolator damping layer. Shock and vibration journal. http://dx.doi.org/10.1155/2014/432760

Das, B. M. (2013). Advanced soil mechanics.CRC Press.

Seed, H. B., Wong, R. T., Idriss, I. M., &Tokimatsu, K. (1986).Moduli and damping factors for dynamic analyses of cohesionless soils. Journal of Geotechnical Engineering, 112(11), 1016-1032.

Griffin, M. J. (2012). *Handbook of human vibration*.Academic press.

Garnier, J., Gaudin, C., Springman, S. M., Culligan, P. J., Goodings, D. J., Konig, D., ...&Thorel, L. (2007). Catalogue of scaling laws and similitude questions in geotechnical centrifuge modelling. International Journal of Physical Modelling in Geotechnics, 7(3), 1-23.

Fluent, A. (2009).12.0 User's Guide.User Inputs for Porous Media, 6.